

# The Neanderthal “chignon”: Variation, integration, and homology

Philipp Gunz, Katerina Harvati\*

*Department of Human Evolution, Max Planck Institute for Evolutionary Anthropology, Deutscher Platz 6, D-04103 Leipzig, Germany*

Received 10 May 2006; accepted 31 August 2006

## Abstract

The occipital bun (“chignon”) is cited widely as a Neanderthal derived trait. It encompasses the posterior projection/convexity of the occipital squama and is associated with lambdoid flattening on the parietal. A ‘hemibun’ in some Upper Paleolithic Europeans is thought by some authors to indicate interbreeding between Neanderthals and early modern Europeans. However, ‘bunning’ is difficult to measure, and the term has been applied to a range of morphological patterns. Furthermore, its usefulness in phylogenetic reconstruction and its homologous status across modern and fossil humans have been disputed. We present a geometric morphometric study that quantitatively evaluates the chignon, assesses its usefulness in separating Neanderthals from modern humans, and its degree of similarity to Upper Paleolithic ‘hemibuns.’ We measured the three-dimensional coordinates of closely spaced points along the midsagittal plane from bregma to inion and of anatomical landmarks in a large series of recent human crania and several Middle and Late Pleistocene European and African fossils. These coordinate data were processed using the techniques of geometric morphometrics and analyzed with relative warps, canonical variates, and singular warps. Our results show no separation between Neanderthals and modern humans, including early modern Europeans, when the shape of the occipital plane midsagittal-profile is considered alone. On the other hand, Neanderthals are well separated from both recent and fossil modern humans when information about the occipital’s relative position and relative size are also included. Furthermore, the occurrence of a highly convex and posteriorly projecting midline occipital profile (interpreted as the occipital bun) is highly correlated ( $>0.8$ ) with a flat parietal midsagittal profile and with antero-superiorly positioned temporal bones across both our recent and our fossil human samples. We conclude that the shape of the occipital profile alone should not be considered an independent trait, as it is very tightly integrated with braincase shape. Our analysis does not support differences in integration of the posterior midsagittal profile and the cranial base in Pleistocene and recent humans.

© 2006 Elsevier Ltd. All rights reserved.

*Keywords:* Middle Pleistocene; Cranial architecture; Human variation; Geometric morphometrics; Semilandmarks

## Introduction

The occipital ‘bun,’ or chignon, is one of the most frequently discussed Neanderthal traits. It has been cited widely as a Neanderthal characteristic (Boule, 1911–1913; Thoma, 1965; Hublin, 1978; Stringer et al., 1984; Condemi, 1991a,b; Sergi, 1991; Dean et al., 1998), and has been claimed to be a Neanderthal autapomorphy (Hublin, 1988; Dean et al., 1998; see also Lieberman, 1995). Furthermore, the presence of a weak occipital bun or ‘hemibun’ in some Upper Paleolithic European

(UPE) specimens is considered by some as evidence of continuity or interbreeding between Neanderthals and early modern humans in Europe. This argument is made most strongly for the Central European fossil record and the Mladeč crania (Jelinek, 1969; Genet-Varcin, 1970; Vlček, 1970; Smith, 1982, 1984; Bräuer, 1989; Gambier, 1997; Churchill and Smith, 2000; Wolpoff et al., 2001; Smith et al., 2005). Despite its prominent place in these discussions, the validity of the hemibun as a Neanderthal derived trait and its usefulness in phylogenetic reconstruction have been questioned.

The occipital bun is described variably as a posterior projection or a great convexity of the upper scale of the occipital bone. It is often associated with the presence of a depression of the area around lambda (“lambdoid flattening”) on the

\* Corresponding author. Tel.: +49 34135 50 358; fax: +49 34135 50 399.

*E-mail addresses:* [gunz@eva.mpg.de](mailto:gunz@eva.mpg.de) (P. Gunz), [harvati@eva.mpg.de](mailto:harvati@eva.mpg.de) (K. Harvati).

occipital and parietal bones. The term ‘occipital bun’ has been applied to a range of morphological patterns (Ducros, 1967; Dean et al., 1998) because it is related to several different aspects of posterior cranial morphology. Not only does the ‘bun’ involve a lambdoid flattening, but it is also associated with a flattened parietal and flat nuchal part of the occipital (Ducros, 1967); its posterior projection is expanded laterally in Neanderthals (Churchill and Smith, 2000); and it is manifested in both the exterior and interior aspects of the occipital bone below lambda and above the internal occipital protuberance (Trinkaus and LeMay, 1982; Lieberman et al., 2000a). This morphology is difficult to assess using either traditional caliper measurements (Ducros, 1967; Dean et al., 1998; Lieberman et al., 2000a) or landmark-based geometric morphometrics methods (Yaroch, 1996; Harvati, 2001), and is therefore usually described qualitatively.

Authors disagree over the distinction between the Neanderthal occipital bun and bunning morphology sometimes present in recent and Upper Paleolithic modern humans. Ducros (1967) attempted to describe the chignon metrically using a complex method for measuring the depth of the lambdoid depression. He concluded that the Neanderthal ‘chignon’ differs from the ‘hemibun’ shown by modern human crania, including Upper Paleolithic specimens; the former was found to describe a relatively smooth curve on the parietal and occipital and to be formed by a general antero-posterior elongation of the cranium and of the occipital bone. In this morphology, the occipital plane seems to be pointing backwards, as it is delimited superiorly by a flat parietal and inferiorly by a flat nuchal plane. In contrast, Ducros (1967) found that modern human and Upper Paleolithic ‘bunning’ was characterized by a ‘saddle-like’ depression of the posterior cranial profile in the area surrounding lambda.

Later metric analyses have not come to conclusive results. In her metric study of occipital bone morphology of fossil and modern humans, Spitz (1985) found the posterior projection of the Neanderthal occipital plane to be strong, but within the modern human range of variation. Yaroch (1996), using the geometric morphometric method of thin-plate splines based on two-dimensional (2-D) landmarks (collected from photographs in lateral view), found that Neanderthals do not show marked occipital plane curvature relative to modern humans. She concluded that the Neanderthal occipital bun is part of the overall antero-posterior elongation of the Neanderthal cranium, and that the Neanderthal occipital plane curvature is not significantly different from that of some recent human groups (but see Friess, 2000). In contrast to Yaroch’s (1996) results, a more recent study by Harvati (2001; see also Reddy et al., 2005) found a strong difference between Neanderthals and modern humans in an analysis of two-dimensional semilandmarks describing the posterior midsagittal profile (bregma to inion) of recent and fossil humans.

The occipital bun morphology has also been assessed from a developmental perspective. Trinkaus and LeMay (1982) pointed out that the expression of bunning forms a continuum that is not easy to dichotomize into ‘present’ or ‘absent’ states, and that it is sometimes found in some

degree among recent humans and in Pleistocene hominins other than Neanderthals. These authors suggested that occipital bun formation is related to the cerebral growth relative to the formation of the vault bones and to the closure of the vault sutures. They questioned the validity of this trait as a phylogenetic character and proposed that its high frequency among Late Pleistocene humans may be explained by other factors, such as a predominance of males in the fossil record, a delayed brain growth pattern, and a relatively large brain size. Lieberman (1995) agreed with Trinkaus and LeMay (1982) that the formation of a bun is probably related to the rate of posterior brain growth relative to timing of the formation of the vault. He proposed that this trait is a convergent, epigenetic character resulting from a combination of large cranial capacities and narrow braincases. In a later study, Lieberman et al. (2000a) tested this hypothesis in a geographically diverse recent human sample and a limited number of Upper Paleolithic and Neanderthal specimens, using a series of linear ecto- and endocranial measurements. Their results indicated that the interaction between cranial base breadth and brain size influenced the degree of occipital bunning in modern humans. Neanderthals, however, were found to differ from modern humans in their combination of wider cranial bases, marked buns, and in their more pronounced degree of internal posterior projection. The authors tentatively concluded that bunning in Neanderthals and Upper Paleolithic Europeans is not homologous, and therefore, its presence in the latter does not indicate genetic continuity. However, they cautioned that their analysis did not include the Central European Upper Paleolithic crania most often cited as showing ‘hemibuns.’

In the present study we had two goals. Firstly, we aimed to quantitatively evaluate the chignon morphology and assess its usefulness in separating Neanderthals from modern humans and from other Pleistocene hominins using geometric morphometric methods and a larger modern and fossil human comparative sample than previously employed. More specifically, we wanted to assess the degree of similarity of the Late Paleolithic ‘hemibuns’ to the Neanderthal occipital buns. As the different aspects of bunning morphology are difficult to capture with a single metric, we used the complete midsagittal profile of the external aspect of the occipital squama and lambdoid area that outlines the occipital bun in lateral view. This profile was quantified by 3-D coordinates along the midsagittal curve in a large sample of recent and Middle-Late Pleistocene humans. Geometric morphometrics of the midsagittal curve enabled us to quantify the continuous variation in the expression of this morphology. Because a flat parietal and cranial base have been linked with Neanderthal occipital buns (Ducros, 1967), we also measured landmarks and semilandmarks on the parietal midsagittal profile and temporal bones on both sides.

Our second goal was to test Lieberman et al.’s (2000a) hypothesis that Neanderthals and modern humans exhibit different patterns of cranial integration resulting in non-homologous posterior cranial projection. Although the methods for quantifying developmental and functional interaction between different

anatomical parts go back at least to the seminal work of Olson and Miller (1951, 1958), little actual research was done in the general field of anthropology until the work of Cheverud and colleagues (Cheverud, 1982, 1988, 1995, 1996; Ackermann and Cheverud, 2000; Marroig and Cheverud, 2001; Marroig et al., 2004) and more recently of other authors in the fields of primate evolution and paleoanthropology (Lieberman et al., 2000a,b, 2002; Ackermann, 2002, 2003, 2005; Bookstein et al., 2003; Polanski and Franciscus, 2003, 2006; Bastir and Rosas, 2004a,b). Here we explored the co-variation of the shape of the posterior vault and the cranial base on the expression of occipital bunning in our combined recent and fossil human sample using the method of singular warps proposed by Bookstein et al. (2003). The bilateral temporal bone landmarks also served as a proxy for cranial base breadth, the variable found by Lieberman et al. (2000a) to be strongly correlated with occipital bunning.

We present two consecutive analyses of landmark-coordinate data:

- (1) As a first step we quantified shape variability using a set of homologous points (semilandmarks) along the posterior midsagittal profile of the upper scale of the occipital bone. We conducted a principal components analysis and a canonical variates analysis on the posterior midline profile from just above lambda to inion, representing the lateral outline of the chignon, to assess how well this morphology separates modern humans from Neanderthals. It is difficult to reconcile the concepts of discrete traits and derived/primitive characters used in cladistics with morphometric analyses of continuous variation, so there is no accurate translation from the language of cladistics to the language and concepts of geometric morphometrics (see also Bookstein, 1994, and Rohlf, 1998 for even more pessimistic views on this subject). However, if the “chignon” were indeed a derived Neanderthal trait, then one would expect to find dimensions in shape space where there is little or no overlap between Neanderthals and recent modern humans or earlier/African fossil specimens. Alternatively, in a somewhat milder version which would allow for some overlap of shape variability, Neanderthal specimens would be expected to cluster on the fringes of modern human variation.
- (2) Our second analysis looked at the morphological integration of the midsagittal profile of the upper scale of the occipital bone with the shape of the temporal bone and of the midsagittal profile of the parietal bone. Using a method called “singular warps” (Bookstein et al., 2003, see next section) we compared the integrational patterns of anatomically modern *Homo sapiens* (AMHS) and archaic *Homo* (including Neanderthals). If modern humans and Neanderthals differed in their pattern of cranial integration, and hence did not share homologous occipital buns, as suggested by Lieberman et al. (2000a), the two groups would not follow the same predictions of occipital shape based on the shape of the cranial vault and base.

## Materials and methods

### Samples

This study included a large modern human sample ( $n = 326$ , Table 1) and several Middle and Late Pleistocene fossil human specimens. The modern human comparative sample comprised 10 regional groupings from a wide geographical range, including an Iberomaurusian series from Afa-lou and Taforalt (North Africa), dated to 14–8.5 ka (Lahr, 1996). In some instances, subsamples of Howells’ (1973, 1989) populations were used. Only adult crania were included, as determined by a fully erupted permanent dentition. Sex was unknown in most cases and was assessed by inspection during data collection and following Howells’ sexing assignments. When possible, equal numbers of male and female specimens were measured.

The fossil sample included 10 Neanderthal specimens from Europe and the Near East; 3 European Middle Pleistocene (MPE) specimens; 10 Middle-Late Pleistocene fossils from Africa and the Near East (MLPA); and 10 Upper Paleolithic anatomically modern humans from Europe and the Near East (UP) (Table 1). Some of the fossils were only complete enough to be included in parts of the first, but not the second, analysis (see Table 1). In the few cases where the original fossils were unavailable, high quality casts or stereolithographs from the Anthropology Departments of the American Museum of Natural History and of New York University were measured.

### Data

Data were collected as 3-D coordinates of anatomical landmarks on the temporal (both sides), parietal, and occipital bones as well as semilandmarks along the midsagittal from bregma to inion. As most fossil specimens did not preserve a complete nuchal plane, the analysis did not include any landmarks or semilandmarks in this region (e.g., opisthion). All crania were measured by one observer (KH) using a Microscribe 3DX digitizer. Each cranium was measured in two orientations that were later superimposed using four fiducial points. The midsagittal profile was digitized as closely spaced points along the curve, which were then resampled to yield equal point count on every specimen. This was achieved by interpolating the original coordinates using cubic splines and resampling segments of this curve between two anatomical landmarks to obtain the same number of equidistantly spaced semilandmarks for each individual. Because morphometric analyses do not accommodate missing data, and because many of the fossil specimens were incomplete, some data reconstruction was necessary. During data collection, and only for specimens with minimal damage, landmarks were reconstructed using anatomical information from the preserved surrounding areas. In cases where bilateral landmarks were missing on one side only, they were estimated by reflected relabeling (Mardia and Bookstein, 2000; see Gunz, 2005 regarding application to missing data). This approach does not require the definition of a midsagittal plane; incomplete

Table 1  
Fossil and recent human samples included in the analysis

Fossil humans	( <i>n</i> = 33)
‘Classic’ and Early Neanderthals	( <i>n</i> = 10)
Amud 1	
Biache*+	
Guattari 1	
La Chapelle-aux-Saints	
La Ferrassie 1	
La Quina 5	
Saccopastore 1	
Shanidar 1*	
Spy 1 and 2	
Middle Pleistocene European Pre-Neanderthals (MPE)	( <i>n</i> = 3)
Petralona+	
Reilingen	
Sima de los Huesos 5*	
Middle-Late Pleistocene African and Near Eastern fossil humans (MLPA)	( <i>n</i> = 10)
Aduma+	
Kabwe	
Ndutu	
Ngaloba	
Omo 1+ and 2	
Qafzeh 6 and 9	
Skhul 5	
Singa	
Eurasian Upper Paleolithic specimens (UP)	( <i>n</i> = 10)
Abri Pataud	
Chancelade*	
Cioclovina	
Cro Magnon 1, 2 and 3+	
Ein Gev	
Mladeč 1 and 5	
Předmostí 3* and 4*	
Recent humans	( <i>n</i> = 326)
1. African ( <i>Mali, Kenya</i> )	( <i>n</i> = 36)
2. Iberomaurusian ( <i>Afalou, Taforalt</i> )	( <i>n</i> = 26)
3. Andaman ( <i>Andaman Islands</i> )	( <i>n</i> = 30)
4. Asian ( <i>North China, Thailand</i> )	( <i>n</i> = 38)
5. Australian ( <i>South Australia</i> )	( <i>n</i> = 32)
6. Inuit ( <i>Alaska, Greenland</i> )	( <i>n</i> = 42)
7. European ( <i>Austria, Greece, Italy, Germany, Yugoslavia</i> )	( <i>n</i> = 45)
8. Khoi-San ( <i>South Africa</i> )	( <i>n</i> = 28)
9. Melanesian ( <i>New Britain</i> )	( <i>n</i> = 30)
10. Middle Eastern ( <i>Syria</i> )	( <i>n</i> = 19)

\* Asterisks indicate specimens for which casts or stereolithographs were used.

+ Plus signs indicate specimens that were only complete enough to be included in the occipital (semi)landmarks analysis.

specimens are least-squares superimposed with their reflected configurations in Procrustes space, and missing data are reconstructed from their homologous counterparts on the other side. In limited instances, points missing on both sides of the cranium or on the midsagittal plane were estimated by minimizing the bending energy of the thin-plate spline between the incomplete specimen and the sample Procrustes average, following Gunz (2005). This missing data protocol decreases the small biological variance due to fluctuating asymmetry

of specimens; all analyses presented here focused only on large scale features.

The semilandmarks were iteratively allowed to slide along the midsagittal curve to minimize the bending energy of the thin-plate spline interpolation function computed between each specimen and the sample Procrustes average. We used the algorithm of Bookstein (1997; see also Gunz et al., 2005) that allows points to slide along tangents to the curve. These tangents were approximated for each semilandmark by converting the vector between the two neighboring points to unit length. Missing points were allowed to slide without constraining them to the curve (‘full relaxation’). Spline-relaxation removes the effects of ‘digitizing error’ in the tangent direction that results from the practical necessity of having to place the semilandmarks somewhere along the curve. After relaxation these semilandmarks can be treated in multivariate analyses as if they had been homologous points in the first place (Bookstein, 1997; Bookstein et al., 1999; Gunz et al., 2005). The landmarks and slid semilandmarks were converted to shape coordinates by Procrustes superimposition (GPA: Gower, 1975; Rohlf and Slice, 1990). This procedure removes information about location and orientation from the raw coordinates and standardizes each specimen to unit centroid size, a size-measure computed as the square root of the summed squared Euclidean distances from each landmark to the specimen’s centroid (Dryden and Mardia, 1998).

For the purposes of our analysis, the landmark and semilandmark data were partitioned into three blocks: occipital, parietal, and temporal (Table 2, Fig. 1). The ‘occipital bone block’ included the landmarks and semilandmarks defining the posterior midline cranial profile from lambda to inion, with the addition of two semilandmarks above lambda on the midsagittal plane of the parietals. The latter points were included because lambdoid flattening on the parietals as well as on the occipital bone is often associated with bunning. The shape of this depression has been argued by Ducros (1967) to differentiate between the morphology of the Upper Paleolithic and other modern human specimens exhibiting a ‘hemibun,’ and the Neanderthal occipital bun. The ‘parietal bone block’ included the landmarks and semilandmarks defining the posterior midline profile from bregma to just above lambda. Finally, the ‘temporal bone block’ included landmarks on the basicranial portion of both right and left temporal bones (see Table 2). The position of the landmarks on the temporal bones relative to the parietal and occipital block serves as a proxy for the orientation of the nuchal plane on which we did not collect measurements (see above); the temporal landmarks were measured on both sides in order to include information about the width of the cranial base.

All analyses were conducted using the 3-D shape coordinates, with the exception of the analysis of occipital shape alone (Fig. 2a,d, see below), for which the coordinates were converted into two dimensions. We projected the posterior midline profile onto the plane spanned by the first two eigenvectors of the coordinates’ variance-covariance matrix; then the semilandmarks were allowed to slide along the curve again to minimize the bending energy between each specimen and

Table 2

Landmarks collected on the temporal, parietal, and occipital bones. See also Fig. 1. Following Harvati 2001, 2003a

<i>Temporal block (L + R)</i>	18
Porion	
Auriculare	
Mastoidale	
Stylomastoid foramen	
Most postero-lateral point of the jugular fossa	
Lateral origin of the petro-tympanic crest	
Most medial point of the petro-tympanic crest at the level of the carotid canal	
Most inferior point on the juxtamastoid crest	
Deepest point of the lateral margin of the articular eminence (root of the articular eminence)	
<i>Parietal block</i>	19
Bregma	
<i>Occipital block</i>	18
Lambda	
Inion	

an iteratively updated Procrustes average. Thus, we eliminated the effect of the parietal and temporal landmarks and semilandmarks in order to study the shape of the posterior occipital profile alone. Because two midsagittal semilandmarks above lambda were assigned to the ‘occipital block,’ the occipital curve was not delimited by anatomical landmarks at its superior end. To calculate a tangent for the free-floating semilandmark, we used *three* semilandmarks above lambda, treated the most superior one as missing during sliding, and later dropped this point before the analysis.

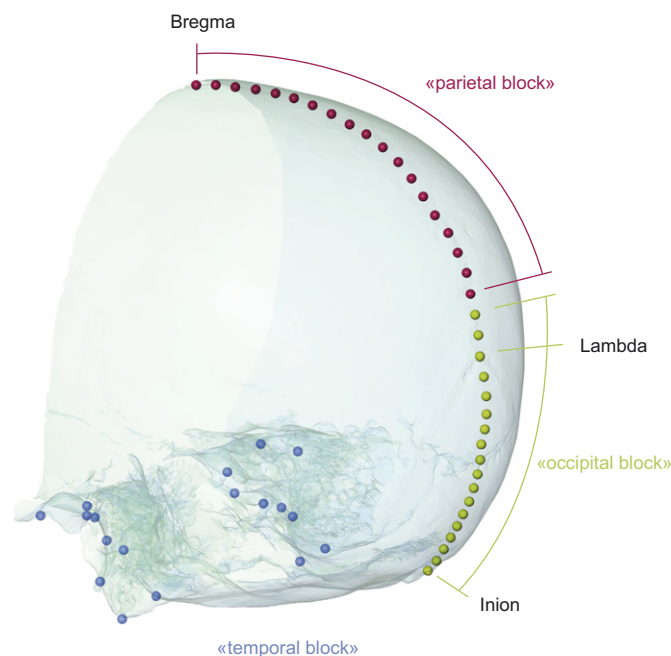


Fig. 1. Landmarks and semilandmarks used in this analysis. For the singular warps analysis, the set of landmarks and semilandmarks was partitioned into three blocks: temporal (blue), occipital (green), and parietal (red). Note that the ‘occipital block’ includes two semilandmarks above lambda to capture lambdoid flattening.

## Analyses

Three statistical methods were used: relative warps analysis, canonical variates analysis, and singular warps analysis.

1. Relative warps: For our first analysis we calculated relative warps (principal component analysis of shape coordinates: Bookstein, 1991; Rohlf, 1993) of landmarks and semilandmarks after Procrustes superimposition. This procedure is an eigen-decomposition of the variance-covariance matrix of Procrustes coordinates. The eigenvectors provide new orthogonal coordinate axes; the projections onto these axes (Fig. 2) are often called ‘relative warp scores.’
2. Canonical variates analysis (CVA): The CVA was computed for the first seven principal components of the Procrustes shape coordinates of the landmarks and semilandmarks (these PCs explain ~95% of the total variation) using *population* as the grouping variable. The Neanderthal specimens were treated as one population; the UP, MPE, and MLPA fossils were not used for the calculations of the canonical axes, and instead plotted in the space of the modern human groups and Neanderthals. The CVA was computed as linear discriminants in the software package ‘R.’
3. Singular Warps for Morphological Integration: Morphological integration of the temporal and the midline profiles of the parietal and occipital bones were studied using the method of singular warps introduced by Bookstein et al. (2003). Singular warps are a special case of partial least squares (PLS; cf. Bookstein et al., 1996; Rohlf and Corti, 2000) used to quantify and visualize the covariation of anatomical regions when all variable blocks are shape coordinates. Blocks of landmarks are defined *a priori*; then the linear combinations of the original shape variables that provide the best mutual cross-prediction between these landmark-blocks are calculated. The algebra is simple with two blocks of variables, where the problem can be solved by a singular value decomposition of the cross-block covariance matrix. In the present case, we studied the interaction of three landmark blocks by applying the iterative algorithm suggested by Bookstein et al. (2003). The analysis yields low-dimensional linear relationships between two or more high-dimensional measurement blocks. To calculate the higher singular warps, we regressed the first singular warp out of the Procrustes shape coordinates and applied the algorithm to the regression residuals (here the higher singular warps are not orthogonal to the first as vectors, as in the in the 2-block case, but instead their *scores* are uncorrelated as scalars). Partitioning the midsagittal curve into two blocks at an arbitrary cutoff point could potentially bias the results because correlations among points are introduced by sliding them together on the same curve. In addition to the three-block analysis, we therefore also computed a two-block singular warp analysis of the temporal landmarks versus the complete midsagittal profile. The results were virtually identical, so only the results of the three-block analysis are described here.

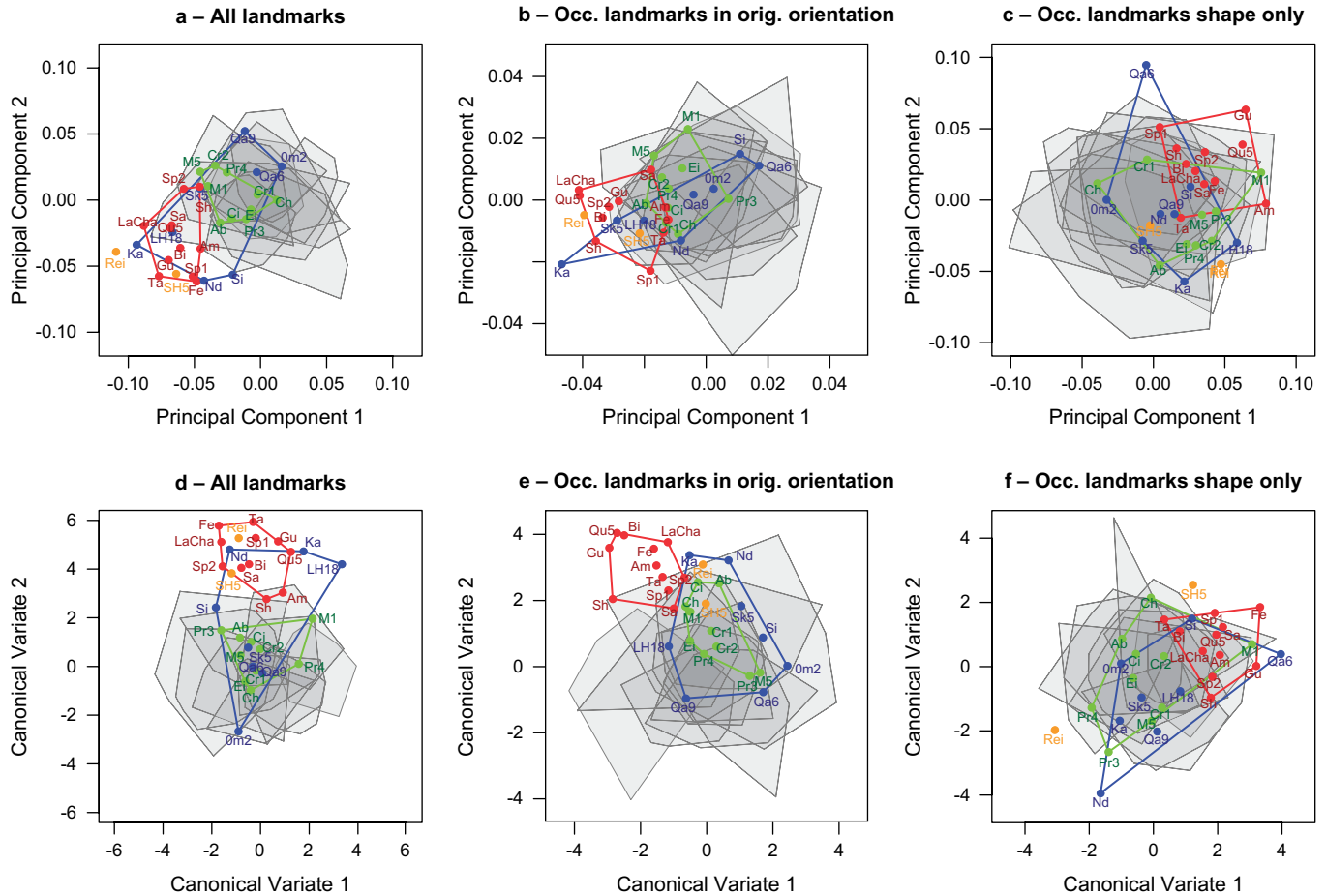


Fig. 2. PCA (a–c) and CVA (d–f) scores. (a) Scores of the first two principal components of the full coordinate set. (b) PC 1 versus 2 of the occipital landmarks and semilandmarks in their original orientation relative to the parietal and temporal bone. (c) PC 1 versus 2 of the occipital landmark and semilandmark shape *alone*. Each fossil specimen is represented by a small dot. Convex hulls are drawn for each group, and both dots and polygons are color-coded (red for Neanderthals, orange for MPE, blue for MLPA, green for UP, and grey for modern humans). Note that the polygons almost completely overlap in the relative warp analysis of occipital shape (c). However, in the analysis that also captures information about the orientation of the occipital profile (b), there is a mean difference between modern humans and Neanderthals in the PC 1 scores, and almost complete separation in the full coordinate set (a). In CVA scores 1 versus 2, archaic *Homo* and Neanderthals are almost completely separated when all landmark and semilandmark data are used (d), and when the occipital profile and relative position are considered together (e). In CVA of occipital shape only (f), it is not possible to find a projection that separates modern and fossil humans; all fossil humans are embraced by modern variation.

Singular warps are linear combinations of the original shape variables and can be visualized either as scores (i.e., projections of the original variables onto these axes; Fig. 3) or as deformations. Bookstein et al. (2003) used thin-plate spline deformation *grids* to visualize their 2-D data; as such grids are inconvenient in three dimensions, we use the thin-plate spline algebra to deform a triangulated scanned *surface* of a single specimen (Fig. 4). The landmarks and semilandmarks of this specimen are used to warp the surface points from the original configuration in Procrustes space into this configuration with different multiples of the singular vectors added. This allows the simultaneous visualization of the morphological changes associated with all three data blocks. Note that the surface areas where there is no (semi)landmark information are just smoothly warped according to the thin-plate spline interpolation.

For data processing and analyses (with exception of the CVA, see above) we used software routines written in

Mathematica (© Wolfram Research) by PG together with Philipp Mitteroecker (University of Vienna). Visualization of the singular warps was rendered in Amira (© Mercury Computer Systems S.A.).

## Results

### Relative warps analysis

Figure 2a–c contrast the relative warps (principal components) of the complete landmark/semilandmark set (Fig. 2a) with two subtly different principal components (PC) analyses of the landmarks and semilandmarks of the ‘occipital block,’ calculated from two different sets of Procrustes shape-coordinates. Figure 2b shows the first two PCs of the occipital landmarks and semilandmarks, but in their original orientation relative to the parietal and temporal bone. To achieve this, the landmarks on the temporal bones and the (semi)landmarks

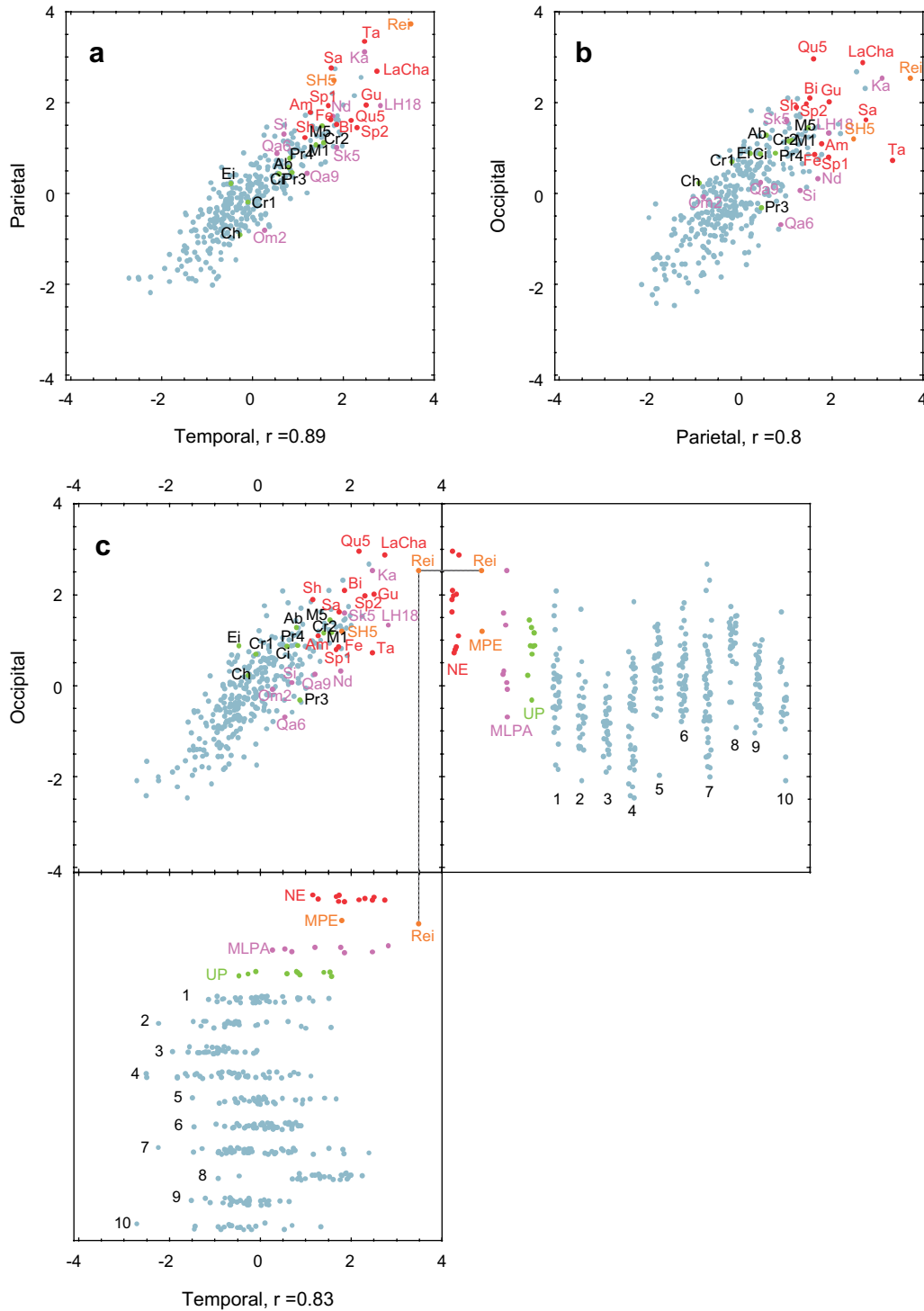


Fig. 3. Singular warp scores of the three coordinate blocks plotted against each other. These plots show how well one can predict the shape of one block from the other block. NE and MPE crania have higher scores than most modern humans for all blocks, but the integrational pattern is the same between groups. (c) Temporal and occipital scores are plotted for each group separately to demonstrate the considerable variability within geographic groups. Dashed grey lines are drawn to connect the scores of 'Reilingen' to show how this panel should be read. The color-coding is the same as in Fig. 1, with the exception of the MLPA, which is here coded in purple. The numbers in (c) correspond to the order of modern human populations in Table 1.

on the midline of the parietal were used in the Procrustes superimposition step, but not included in the PCA, which was calculated only from the subset of occipital (semi)landmarks. Finally, Fig. 2c shows the scores of the first two principal

components of the occipital shape coordinates after spline relaxation and Procrustes superimposition of this dataset *alone* (thus representing *shape* but not relative position/orientation). Therefore, while Fig. 2c visualizes the main directions of

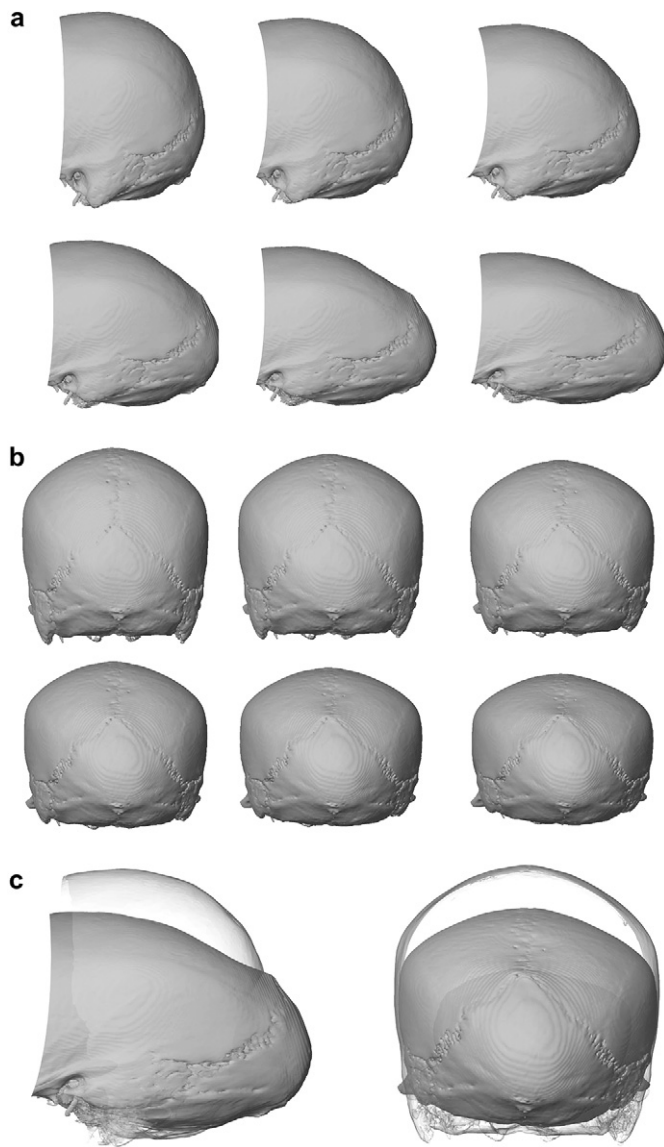


Fig. 4. First singular warp. The shape dimensions associated with the scores shown in Fig. 3 can be visualized together. Here a modern human cranium's surface is deformed by adding the different multiples of the singular vectors to the Procrustes coordinates of this particular specimen and shown in (a) lateral and (b) posterior view. (c) Start (translucent surface) and endpoint of this sequence superimposed. In effect, this morph visualizes the shape-change associated with going along the grey line from the center of the scores plots of Fig. 3 to the upper right corner. The first singular warp contrasts a globular cranial shape with a more elliptical shape. Note that as occipital bunning increases, the cranial width does not change at all; the temporal bones get more superiorly and anteriorly placed and the mastoid decreases in size.

variability of the *shape* of the occipital plane alone, the analysis shown in Fig. 2b includes this shape information along with information about *its position and size relative to the parietal and temporal bones*. Color-coded convex hulls (see figure legend) are drawn for each group (and modern human populations); the individual scores are only plotted for the fossil specimens and omitted for the modern humans to make the figure more readable. When the landmarks and semilandmarks on the occipital, temporal, and parietal bones were analyzed together, Neanderthals and modern humans were almost

completely separated by the first principal component: only Shanidar 1 and Spy 2 fell within the range of modern human variation, and two modern human crania plotted very close to the Neanderthal cluster (Fig. 2a).

The convex hulls overlapped greatly in the first two PCs of both occipital plane analyses (accounting for ~67% and ~85% of the total variation respectively; Fig. 2b, c). The overlap is almost complete in the first relative warp analysis of occipital plane shape. However, in the analysis that also captures information about the orientation of the occipital profile (Fig. 2b), there is a mean difference between modern humans and Neanderthals in the PC 1 scores. Although they fall within the modern human range of variation, all Neanderthals have high scores on PC 1. Some Upper Paleolithic individuals also show high PC 1 scores, but the remaining fossil specimens are well within the recent human variation.

We tested the significance of the group mean differences between Neanderthals and all other groups listed in Table 1 using a permutation test (Good, 2000); MPE were not included in this analysis because this group is only represented by two specimens. The observed Procrustes distance between group means was compared with 8,000 permutations where the group labels were randomly reassigned. The  $p$  value was then calculated as the number of cases the randomly reassigned group mean differences exceeded the actually observed value, divided by 8,001 (the number of permutations plus the original calculation). We computed the Bonferroni corrected  $p$  values for these 12 pairwise comparisons for the shape space with the greatest overlap—occipital shape only (Fig. 2c). Despite the apparent overlap in the scores of the first two PCs, group mean differences in complete Procrustes space were highly significant for all modern groups with the exception of modern Africans ( $p \sim 0.05$ ), and not significant for UP and the pooled Afalou and Tavoralt sample.

#### Canonical variates analysis

Figure 2d–f show the first two canonical variates for the three CVAs conducted on the same landmark and semilandmark sets as in Fig. 2a–c. Whereas relative warps analysis provides new coordinate axes that maximize the variance irrespective of group membership, CVA tries to find dimensions in shape space that maximize the ratios of the between-groups to the within-groups distances. It is evident that when the shape of the occipital profile was considered alone (Fig. 2f), it was not possible to find a projection that separated modern and fossil humans; all fossil humans were embraced by modern variation. When the occipital profile and relative position were considered together, or when all landmark and semilandmark data were used (Fig. 2d–e), European archaic *Homo* and Neanderthals were almost completely separated from modern humans, including the UP. On the other hand, the Qafzeh/Skhul specimens, as well as Singa and Omo 2 (but not Kabwe, Ndutu or LH 18), fall within the modern human range of variation along these axes.

### Singular warps

Singular warps analysis provides separate descriptions of the parietal, occipital, and temporal bone coordinates and the relations among these three blocks. The relationships of the first singular warp ( $\sim 30\%$  of the total variation) are plotted as singular warp scores in Fig. 3; the singular vectors themselves are shown as a surface-morph in Fig. 4.

The score-plots show how well shape and position of one landmark block can be predicted by shape and position of the other (and vice versa; a perfect correlation would result in all points falling on the grey diagonal). All three scores are highly correlated (temporal-parietal:  $r \sim 0.89$ , parietal-occipital:  $r \sim 0.8$ , temporal-occipital:  $r > 0.83$ ). The panels in Fig. 3a–c show the same consistent pattern: while Upper Paleolithic *Homo sapiens* cannot be distinguished from recent humans, most European and some African Middle-Late Pleistocene *Homo* fall outside the range of modern variation for temporal and parietal scores; overlap is greater in the occipital scores. These scores of the first singular warp are not correlated with log centroid size ( $r < 0.02$  for all three scores). The higher singular warps were calculated but are not discussed here, as their scores show no separation between modern and fossil humans, and the associated shape dimensions are not related to occipital bunning. The first three singular warps explain  $\sim 80\%$  of the total variance; higher singular warps show only small-scale effects like asymmetry. Furthermore, in the scores-plots of the second and third singular warps, fossil and modern humans lie along the same trajectories (plots not shown).

Figure 3c also shows the temporal and occipital scores separately for each group (points are ‘jittered’ to avoid overplotting). It is evident that variation within extant geographic groups is considerable for the temporal and occipital scores—the same is true for the parietal scores (not shown). However, while Neanderthals and archaic *Homo* consistently have higher scores than most modern humans (so there is an apparent mean difference), they follow the same linear trend when the different blocks are viewed together. This result points to a shared pattern of integration for these cranial regions in modern and fossil humans.

The shapes associated with these three axes are visualized in Fig. 4: the occurrence of a highly convex and posteriorly projecting occipital profile (interpreted as the occipital bun) is highly correlated ( $>0.8$ ) with a flat parietal midline profile and with anteriorly and superiorly positioned temporal bones. It is interesting to point out that the detailed shape of the temporal bone is not affected—it is rather the relative position of this bone that is important here. This result did not change when singular warps were calculated only for the modern human sample: posterior projection of the occipital midline is correlated with a flat parietal midline and temporal bones that are placed anteriorly and superiorly (results are not shown here). We also computed the singular warps for the fossil specimens alone, to check whether the excess of modern specimens in the pooled analysis would impose the modern integrational pattern upon the fossils.

In essence, the results described for the pooled analysis stay the same; in the fossil sample, the shape-changes described above for the pooled analysis are captured by the first two singular warps: the first singular warp is driven by the correlation of a flat parietal midline with a relatively wide cranial base ( $r \sim 0.82$ ); the second singular warp entails posterior projection of the occipital midline, an anteriorly and superiorly positioned cranial base, and a relatively anterior placement of bregma (all three correlations higher than  $r > 0.74$ ).

### Discussion

#### Defining the occipital bun

These analyses indicate that the midline shape of the occipital squama and lambdoid area, when considered alone, does not distinguish Neanderthals or other fossil hominins from recent humans even in the CVA, an analysis designed to maximize separation between groups (Fig. 2c, f). Although the mean Neanderthal scores on these axes are significantly different from most modern human groups, they are clearly encompassed within the range of modern human variation. When the orientation of the occipital plane is also taken into account (Fig. 2b, e) separation is better, and when the full dataset of occipital, parietal, and temporal bone landmarks and semilandmarks is used, an almost full separation was achieved between Neanderthals and modern humans. It is evident that the convexity of the occipital squama and the flattening of the lambdoid region are not the salient features of Neanderthal ‘buns,’ and do not greatly contribute to the metric separation of modern humans and Neanderthals demonstrated by numerous previous studies (e.g., Stringer, 1974, 1992; Howells, 1989; Bräuer, 1992; Harvati, 2003b; Harvati et al., 2004). Instead, it is the combination of occipital squama convexity/lambdoid flattening with occipital bone orientation relative to the rest of the cranium that differentiates Neanderthals from modern humans.

Our results also indicate a very tight integration pattern among the midline shape of the occipital squama and the shape and relative position of the parietal bone and cranial base. This result strongly suggests that the midsagittal shape of the occipital plane profile should not be considered an independent trait, as it is so tightly integrated with braincase shape.

Our findings reconcile the observation of marked occipital buns in Neanderthals with the metric results obtained by Spitzky (1985) and Yaroeh (1996), who found the Neanderthal occipital plane curvature to lie within the limits of modern human variation. They are also consistent with previous findings of strong separation between Neanderthals and modern human based on semilandmark analyses of the midline profile of the parietal and occipital bones (Harvati, 2001; Reddy et al., 2005).

It is worth pointing out, however, that the present study addresses only some of the aspects of cranial morphology linked to the occipital bun. Aspects not addressed here include the lateral expansion of the occipital plane curvature and its strong endocranial posterior projection. Therefore,

the possibility remains that when these additional features of the occipital bone are taken into account, Neanderthals and modern humans can be distinguished more readily. Weber et al. (2006) presented a morphometric PCA analysis of a similar dataset, focusing on the phylogenetic affinities of the Mladeč crania, using surface semilandmarks covering the entire neurocranium. These authors found that when lateral semilandmarks on the posterior vault and size information are included, Neanderthals are separated better from modern humans in the PCA (albeit still not as well as in other cranial regions).

#### *Upper Paleolithic and other Pleistocene hominins*

The midsagittal convexity of the occipital squama and lambdoid area does not differentiate Neanderthals from modern humans at all. The group mean of the UP sample was not significantly different from that of Neanderthals, but neither was that of the African or the Afalou/Taforalt samples. Therefore, this is unlikely to hint at a special phylogenetic relationship between Neanderthals and UP. In the analyses that did separate Neanderthals from modern humans (PCA and CVA of shape plus relative position of occipital squama; singular warps analysis), the UP did not fall with Neanderthals. The European pre-Neanderthal specimens, however, as well as some African Middle Pleistocene fossils, did (e.g., Kabwe, Ngaloba). There was a great deal of variation among the African and Near Eastern fossils, likely related to the great geographic and time range spanned by this sample, with the Qafzeh and Omo 2 specimens showing the most modern human-like pattern. The small sample size of the available European pre-Neanderthal fossil record precludes any definitive conclusions in this regard.

#### *Patterns of integration and homology*

The results of our singular warps analysis indicate that occipital bunning in modern humans and Neanderthals alike is associated with anteriorly and superiorly placed temporal bones/cranial bases and a flat parietal midline (Fig. 4).

The tight morphological integration between parietal, temporal, and occipital bones is evident in the high correlations (all higher than 0.8) between the singular warp scores. These correlations are unlikely to be caused by direct individual interactions of the bones; instead they are most likely spurious correlations because all bones are affected by a single factor, brain expansion, during ontogeny. Not only were these integrational patterns found to be tight, but they were also *shared* between modern and fossil humans. While Neanderthals and archaic *Homo* consistently had higher scores than most modern humans, they followed the same linear trend when the different blocks were viewed together. Neanderthals thus have the amount of occipital bunning that one would predict for a human with such a supero-anteriorly positioned cranial base and such a flat parietal. This is particularly apparent in the few modern outliers that have temporal, parietal, and occipital scores similar to archaic humans. The UP specimens

were all within the modern human cloud. Note that—with the exception of the Andamanese (population #3)—along the first singular warp every modern human group has outliers that fall within the Neanderthal variation (Fig. 3c). This includes crania from Africa, Asia, and the Middle East, hence no European pattern can be discerned.

This finding differs from those of Lieberman et al. (2000a) who studied the degree of occipital bunning among recent and fossil humans in relation to endocranial volume and relative to basicranial breadth. These authors found that occipital bunning occurs more frequently in large-brained individuals with narrow skulls, and concluded that in modern humans, ‘bunning’ may be related to the constraints of a dolicocephalic skull with large cranial capacity. Because Neanderthals have wide cranial bases relative to endocranial volume, they suggested that the Neanderthal “chignon” was not homologous with bunning found in modern humans.

We think that the difference in our results stems from differences in the kinds of data used. Lieberman et al.’s (2000a) interpretations are based on partial correlation coefficients calculated from measurements of endocranial volume, from craniofacial linear measurements and from angles and indices derived from the latter. By contrast, we focused only on the external aspects of the posterior vault and cranial base, and did not use direct measurements of endocranial volume. Because our study neglected endocranial and anterior cranial morphology, our results are not directly comparable with those of Lieberman et al. (2000a), and thus, might not be mutually exclusive. Some of the conflicting results in these two studies may also be caused by differences in methodology. Lieberman et al. (2000a) employed partial correlation analysis, in which some variables are held constant (thus partialling out their influence) in order to explore the independent contribution of another variable to the outcome variable. The method is closely related to multiple regression (in fact the multiple regression coefficients are scaled versions of the partial correlation coefficients) and can be plagued by the same problems, as partial correlation coefficients can sometimes be misleading. When the variables themselves are highly inter-correlated, such an analysis may inadvertently result in the partialling out of the main signal in the data. Correlations between cranial measurements are introduced because growth processes influence all measurements at the same time. In the neurocranium, a single factor, namely brain growth, is almost exclusively driving the shape changes of all bones contributing to the brain’s shell.

#### *Developmental integration*

While the cranial base is formed by endochondral ossification of cartilaginous precursors, the calvaria is formed by membranous bones directly from mesenchyme. During early development, the cranium must grow rapidly to keep pace with the expansion of the brain. This is accomplished through two modes of cranial growth: sutural growth and surface growth. During ontogeny, growth occurs predominantly at the margins of these membrane bones, where fibrous tissues form sutures (Henderson et al., 2004). Current knowledge about

the genetic control of sutural growth is based on *in vitro* and *in vivo* experiments with rodents and on the etiology of various forms of craniosynostosis in humans. A regulatory cascade including transforming growth factor beta (TGF-beta), fibroblast growth factor (FGF), the Hox-like gene *MSX-2*, and *TWIST* is involved in the development and maintenance of calvarial sutures (reviewed in Morriss-Kay and Wilkie, 2005).

Cranium and spinal chord form a closed system, hence any increase of volume increases intracranial pressure (Alperin et al., 2000). Henderson et al. (2004) suggested that the tensile forces associated with intracranial pressure are too small to directly influence osteoblast biology. These authors speculated that the dura mater may respond to tensile strain generated by growth of the brain by producing signals for osteoblast proliferation and differentiation, and thereby control the rate of bone deposition in the overlying sutures. This conclusion seems to be supported by the findings of Opperman et al. (1995), who were able to demonstrate that soluble factors expressed by the dura mater were required to maintain suture patency *in vitro*.

The importance of genetic control of brain-case growth is undisputed, but even in highly controlled forms of development, the realization of morphology continues to depend on non-programmatic, epigenetic mechanisms (Newman and Müller, 1999). If a suture ossifies prematurely during times of rapid brain expansion, this often leads to compensatory growth, both in other sutures and by remodeling of other parts of the skull (Morriss-Kay and Wilkie, 2005). Therefore it seems likely that even subtle changes in the timing pattern of suture fusion and/or rate and timing of brain growth would be sufficient to explain the overall differences of brain-case shape we have described here. We thus favor the interpretation of Trinkaus and LeMay (1982) and Lieberman (1995; Lieberman et al., 2000a) that occipital bunning ultimately stems from developmental processes related to the timing of brain and cranial vault growth. Because no pedigree information exists for the human samples we used, there are no means to determine the relative importance of genetic and epigenetic influences on the developmental processes underlying the large variability within modern human geographic groups along all three singular warp scores. Differences in developmental integration patterns between Neanderthals and modern humans have been proposed as evidence to support distinct species status for the former (Lieberman et al., 2000a, 2002; Ponce de León and Zollikofer, 2001). The reverse of course is not true—shared integrational patterns in Neanderthals and modern humans do *not* suggest that these taxa belong to the same species. Different patterns of developmental integration and variation between groups result in non-homologous features whose variation in extant groups cannot be used to assess fossil relationships (Ackermann, 2003, 2005). The present study failed to detect differences in integration of the posterior midline profile with the cranial base between archaic and modern humans, although it is possible that these results would change with the addition of endocranial data. We therefore consider the exterior midsagittal aspect of the Neanderthal ‘chignon’ to be homologous to bunning morphology in modern humans.

## Conclusions

Our results strongly suggest that the shape of the occipital profile/lambdoid flattening should not be considered an independent trait as it is so tightly integrated with braincase shape. The midsagittal profile of the upper scale of the occipital bone, when considered independently of its position and orientation relative to the other vault bones, does not differentiate Neanderthals from modern humans. Discrimination improves when positional information is also taken into account, and even more when the shape of the parietal and temporal bones is also considered. No special relationship was found between Neanderthals and UP specimens. Finally, our findings do not support differences in cranial integration between fossil and modern humans with respect to exterior aspects of occipital bunning: both Middle-Late Pleistocene *Homo* and UP exhibit exactly the amount of bunning predicted based on extant humans given the shape of their parietal and the position of their temporal bone.

## Acknowledgments

We thank all the curators and collections managers in several institutions across Europe, Africa, and the U.S. for kindly allowing access to both fossil and extant material used in this study, and the family of Max Lohest for donating the Spy Neanderthal remains to science. We thank Maximilian v. Harling for the CT scan used to create Figs. 1 and 4. We are also grateful to Jean-Jacques Hublin, Tim Weaver, Zeray Alemseged, Matt Skinner, Fred Bookstein, Philipp Mitteröcker, Susan Antón, Dan Lieberman, and two anonymous reviewers for providing very helpful comments and suggestions. This research was funded in its various stages by grants to KH by the American Museum of Natural History; NYCEP (this is NYCEP morphometrics group contribution No. 21); the Onassis and the CARE Foundations; and the National Science Foundation. Support was also provided by New York University, the Max Planck Society, and the “EVAN” Marie Curie Research Training Network MRTN-CT-019564.

## References

- Ackermann, R.R., 2002. Patterns of covariation in the hominoid craniofacial skeleton: implications for paleoanthropological models. *J. Hum. Evol.* 43 (2), 167–187.
- Ackermann, R.R., 2003. Morphological integration in hominoids: a tool for understanding human evolution. *Am. J. Phys. Anthropol.* 36, 55.
- Ackermann, R.R., 2005. Ontogenetic integration of the hominoid face. *J. Hum. Evol.* 48 (2), 175–197.
- Ackermann, R.R., Cheverud, J.M., 2000. Phenotypic covariance structure in tamarins (genus *Saguinus*): a comparison of variation patterns using matrix correlation and common principal component analysis. *Am. J. Phys. Anthropol.* 111 (4), 489–501.
- Alperin, N.J., Lee, S.H., Loth, F., Raksin, P.B., Lichtor, T., 2000. MR-intracranial pressure (ICP): a method to measure intracranial elastance and pressure noninvasively by means of MR imaging: baboon and human study. *Radiology* 217 (3), 877–885.

- Bastir, M., Rosas, A., 2004a. Facial heights: evolutionary relevance of postnatal ontogeny for facial orientation and skull morphology in humans and chimpanzees. *J. Hum. Evol.* 47 (5), 359–381.
- Bastir, M., Rosas, A., 2004b. Comparative ontogeny in humans and chimpanzees: similarities, differences and paradoxes in postnatal growth and development of the skull. *Ann. Anat.* 186 (5–6), 503–509.
- Bookstein, F.L., 1991. *Morphometric Tools for Landmark Data: Geometry and Biology*. Cambridge University Press, Cambridge.
- Bookstein, F.L., 1994. Can biometrical shape be a homologous character? In: Hall, B.K. (Ed.), *Homology: The Hierarchical Basis of Comparative Biology*. Academic Press, New York, pp. 197–227.
- Bookstein, F.L., 1997. Landmark methods for forms without landmarks: morphometrics of group differences in outline shape. *Med. Image Anal.* 1 (3), 225–243.
- Bookstein, F.L., Gunz, P., Mitteroecker, P., Prossinger, H., Schaefer, K., Seidler, H., 2003. Cranial integration in *Homo*: singular warps analysis of the midsagittal plane in ontogeny and evolution. *J. Hum. Evol.* 44 (2), 167–187.
- Bookstein, F.L., Sampson, P.D., Streissguth, A.P., 1996. Exploiting redundant measurement of dose and developmental outcome: new methods from the behavioral teratology of alcohol. *Dev. Psychol.* 32 (3), 404–415.
- Bookstein, F.L., Schaefer, K., Prossinger, H., Seidler, H., Fiedler, M., Stringer, C.B., Weber, G.W., Arsuaaga, J.L., Slice, D., Rohlf, F.J., et al., 1999. Comparing frontal cranial profiles in archaic and modern homo by morphometric analysis. *Anat. Rec.* 257 (6), 217–224.
- Boule, M., 1911–1913. L'homme fossile de la Chapelle-aux-Saints. *Annl. Paléont.* 6, 11–172; 177, 121–156; 178, 171–170.
- Bräuer, G., 1989. The evolution of modern humans: a comparison between the African and non-African evidence. In: Stringer, C.B., Mellars, P. (Eds.), *The Human Revolution*. Princeton University Press, Princeton, pp. 123–154.
- Bräuer, G., 1992. Africa's place in the evolution of *Homo sapiens*. In: Bräuer, G., Smith, F.H. (Eds.), *Continuity or Replacement: Controversies in Homo sapiens Evolution*. A.A. Balkema, Rotterdam, pp. 83–98.
- Cheverud, J.M., 1982. Phenotypic, genetic, and environmental morphological integration in the cranium. *Evolution* 36 (3), 499–516.
- Cheverud, J.M., 1988. Spatial-analysis in morphology illustrated by rhesus macaque cranial growth and integration. *Am. J. Phys. Anthropol.* 75 (2), 195–196.
- Cheverud, J.M., 1995. Morphological integration in the saddle-back tamarin (*Saguinus fuscicollis*) cranium. *Am. Nat.* 145 (1), 63–89.
- Cheverud, J.M., 1996. Developmental integration and the evolution of pleiotropy. *Am. Zool.* 36 (1), 44–50.
- Churchill, S.E., Smith, F.H., 2000. Makers of the early Aurignacien of Europe. *Am. J. Phys. Anthropol.* 43 (Yrbk), 61–115.
- Condemi, S., 1991a. Neanderthal man, vol 7, extinction – French – Vandermeersch, B. *Anthropologie* 95 (4), 852–853.
- Condemi, S., 1991b. Circeo I and variability among classic Neanderthals. In: Piperno, M., Scichilone, G. (Eds.), *The Circeo 1 Neanderthal Skull: Studies and Documentation*. Istituto Poligrafico e Zecca dello Stato, Rome.
- Dean, D., Hublin, J.J., Holloway, R., Ziegler, R., 1998. On the phylogenetic position of the pre-Neanderthal specimen from Reilingen, Germany. *J. Hum. Evol.* 34 (5), 485–508.
- Dryden, I., Mardia, K.V., 1998. *Statistical Shape Analysis*. John Wiley & Sons, New York.
- Ducros, A., 1967. Le chignon occipital, mesure sur le squelette. *L'Anthropologie* 71, 75–96.
- Friess, M., 2000. Application des “Thin-Plate Splines” en paléanthropologie: nouvelles données et leurs implications pour l'origine de l'homme moderne. In: Andrieux, P., Hadjouis, D., Dambricourt Malassé, A. (Eds.), *L'identité Humaine en Question, Nouvelles Problematiques et Nouvelles Technologies en Paleontologie Biologiques*. Actes du Colloque, Créteil, 26–28 Mai 1999.
- Gambier, D., 1997. Modern humans at the beginning of the Upper Paleolithic in France: anthropological data and perspectives. In: Clark, G.A., Willermet, C.M. (Eds.), *Conceptual Issues in Modern Human Origins Research*. Aldine de Gruyter, New York, pp. 117–131.
- Genet-Varcin, E., 1970. Considérations morphologiques sur l'homme de Cro-Magnon. In: Camps, G., Olivier, G. (Eds.), *L'Homme de Cro-Magnon*. Arts et Métiers Graphiques, Paris.
- Good, P.I., 2000. *Permutation Tests: A Practical Guide to Resampling Methods for Testing Hypotheses*. Springer, New York.
- Gower, J.C., 1975. Generalized Procrustes analysis. *Psychometrika* 40, 33–51.
- Gunz, P., 2005. *Statistical and geometric reconstruction of hominid crania: reconstructing australopithecine ontogeny*. Ph.D. Dissertation, University of Vienna.
- Gunz, P., Mitteroecker, P., Bookstein, F.L., 2005. Semilandmarks in three dimensions. In: Slice, D.E. (Ed.), *Modern Morphometrics in Physical Anthropology*. Kluwer Academic/Plenum Publishers, New York, pp. 73–98.
- Harvati, K., 2001. *The Neanderthal problem: 3-D geometric morphometric models of cranial shape variation within and among species*. Ph.D. Dissertation, City University of New York.
- Harvati, K., 2003a. Quantitative analysis of Neanderthal temporal bone morphology using 3-D geometric morphometrics. *Am. J. Phys. Anthropol.* 120, 323–338.
- Harvati, K., 2003b. The Neanderthal taxonomic position: models of intra- and inter-specific morphological variation. *J. Hum. Evol.* 44, 107–132.
- Harvati, K., Frost, S.R., McNulty, K.P., 2004. Neanderthal taxonomy reconsidered: implications of 3D primate models of intra- and inter-specific differences. *Proc. Natl. Acad. Sci. U.S.A.* 101, 1147–1152.
- Henderson, J.H., Longaker, M.T., Carter, D.R., 2004. Sutural bone deposition rate and strain magnitude during cranial development. *Bone* 34 (2), 271–280.
- Howells, W.W., 1973. *Cranial Variation in Man: A Study by Multivariate Analysis of Patterns of Difference Among Recent Human Populations*. Harvard University Press, Cambridge.
- Howells, W.W., 1989. *Skull Shapes and the Map: Craniometric Analyses in the Dispersion of Modern Homo*. Harvard University Press, Cambridge.
- Hublin, J.J., 1978. Quelques caractères apomorphes du crâne néandertalien et leur interprétation phylogénétique. *Comptes Rendus de l'Académie des Sciences de Paris*. t.287, sér. D: 923–926.
- Hublin, J.J., 1988. Caractères dérivés de la région occipitomasto-dienne chez les Néandertaliens. *L'Anatomie* 3, 67–73.
- Jelinek, J., 1969. Neanderthal man and *Homo sapiens* in central and eastern Europe. *Curr. Anthropol.* 10 (5), 475.
- Lahr, M.M., 1996. *The Evolution of Modern Human Diversity: A Study of Cranial Variation*. Cambridge University Press, Cambridge.
- Lieberman, D.E., 1995. Testing hypotheses about recent human-evolution from skulls – integrating morphology, function, development, and phylogeny. *Curr. Anthropol.* 36 (2), 159–197.
- Lieberman, D.E., McBratney, B.M., Krovitz, G., 2002. The evolution and development of cranial form in *Homo sapiens*. *Proc. Natl. Acad. Sci.* 99 (3), 1134–1139.
- Lieberman, D.E., Pearson, O.M., Mowbray, K.M., 2000a. Basicranial influence of overall cranial shape. *J. Hum. Evol.* 38, 291–315.
- Lieberman, D.E., Ross, C.F., Ravosa, M.J., 2000b. The primate cranial base: ontogeny, function, and integration. *Am. J. Phys. Anthropol.* 43 (Yrbk), 117–169.
- Mardia, K.V., Bookstein, F.L., 2000. Statistical assessment of bilateral symmetry of shapes. *Biometrika* 87, 285–300.
- Marroig, G., Cheverud, J.M., 2001. A comparison of phenotypic variation and covariation patterns and the role of phylogeny, ecology, and ontogeny during cranial evolution of new world monkeys. *Evolution* 55 (12), 2576–2600.
- Marroig, G., Vivo, M., Cheverud, J.M., 2004. Cranial evolution in sakis (*Pithecia*, Platyrrhini) II: evolutionary processes and morphological integration. *J. Evol. Biol.* 17 (1), 144–155.
- Morriss-Kay, G.M., Wilkie, A.O., 2005. Growth of the normal skull vault and its alteration in craniosynostosis: insights from human genetics and experimental studies. *J. Anat.* 207 (5), 637–653.
- Newman, S.A., Müller, G.B., 1999–. *Morphological evolution: epigenetic mechanisms*. Encyclopedia of Life Sciences. John Wiley & Sons, Chichester. <<http://www.els.net/>>.
- Olson, E.C., Miller, R.L., 1951. Relative growth in paleontological studies. *J. Paleontol.* 25, 212–223.

- Olson, E.C., Miller, R.L., 1958. Morphological Integration. The University of Chicago Press, Chicago.
- Opperman, L.A., Passarelli, R.W., Morgan, E.P., Reintjes, M., Ogle, R.C., 1995. Cranial sutures require tissue interactions with dura mater to resist osseous obliteration in vitro. *J. Bone Miner. Res.* 10 (12), 1978–1987.
- Polanski, J.M., Franciscus, R.G., 2003. Conditional independence modeling of neurocranial, facial, and masticatory integration in *Pan*, *Gorilla* and recent *Homo*. *Am. J. Phys. Anthropol.*, 169.
- Polanski, J.M., Franciscus, R.G., 2006. Patterns of craniofacial integration in extant *Homo*, *Pan*, and *Gorilla*. *Am. J. Phys. Anthropol.* 131 (1), 38–49.
- Ponce de León, M.S., Zollikofer, C.P.E., 2001. Neanderthal cranial ontogeny and its implications for late hominid diversity. *Nature* 412 (6846), 534–538.
- Reddy, D.P., Harvati, K., Kim, J., 2005. Alternative approaches to ridge-curve analysis using the example of the Neanderthal occipital bun. In: Slice, D. (Ed.), *Modern Morphometrics in Physical Anthropology*. Kluwer Academic/Plenum Publishers, New York, pp. 99–115.
- Rohlf, F.J., 1993. Relative warp analysis and an example of its application to mosquito wings. In: Marcus, L.F., Bello, E., García-Valdecasas, A. (Eds.), *Contributions to Morphometrics*. Museo Nacional de Ciencias Naturales, Madrid, pp. 131–159.
- Rohlf, F.J., 1998. On applications of geometric morphometrics to studies of ontogeny and phylogeny. *Syst. Biol.* 47 (1), 147–158.
- Rohlf, F.J., Corti, M., 2000. Use of two-block partial least-squares to study covariation in shape. *Syst. Biol.* 49 (4), 740–753.
- Rohlf, F.J., Slice, D., 1990. Extensions of the Procrustes method for the optimal superimposition of landmarks. *Syst. Zool.* 39, 40–59.
- Sergi, S., 1991. The Neanderthal cranium of Monte Circeo (Circeo 1). In: Piperno, M., Scichilone, G. (Eds.), *The Circeo 1 Neanderthal Skull: Studies and Documentation*. Instituto Poligrafico e Zecca dello Stato, Rome.
- Smith, F.H., 1982. Upper Pleistocene hominid evolution in south-central Europe: a review of the evidence and analysis of trends. *Curr. Anthropol.* 23, 667–703.
- Smith, F.H., 1984. Fossil hominids from the upper Pleistocene of Central Europe and the origin of modern Europeans. In: Smith, F.H., Spencer, F. (Eds.), *The Origins of Modern Humans: A World Survey of the Fossil Evidence*. Liss, New York, pp. 211–250.
- Smith, F.H., Janković, I., Karavanić, I., 2005. The assimilation model, modern human origins in Europe, and the extinction of Neanderthals. *Quatern. Int.* 137, 7–19.
- Spitery, E., 1985. Principaux caractères évolutifs de l'os occipital chez les hominidés fossiles. *L'Anthropologie* 89, 75–91.
- Stringer, C.B., 1974. Population relationships of later Pleistocene hominids: a multivariate study of available crania. *J. Archaeol. Sci.* 1, 317–342.
- Stringer, C.B., 1992. Replacement, continuity and the origin of *Homo sapiens*. In: Bräuer, G., Smith, F.H. (Eds.), *Continuity or Replacement: Controversies in *Homo sapiens* Evolution*. A.A. Balkema, Rotterdam.
- Stringer, C.B., Hublin, J.J., Vandermeersch, B., 1984. The origin of anatomically modern humans in Western Europe. In: Smith, F.H., Spencer, F. (Eds.), *The Origins of Modern Humans: A World Survey of the Fossil Evidence*. Liss, New York, pp. 51–135.
- Thoma, A., 1965. La définition des Néanderthaliens et la position des hommes fossiles de Palestine. *L'Anthropologie* 69, 519–534.
- Trinkaus, E., LeMay, M., 1982. Occipital bunning among later Pleistocene hominids. *Am. J. Phys. Anthropol.* 57, 27–35.
- Vlček, E., 1970. Relations morphologiques des types humains fossiles de Brno et Cro-Magnon au Pleistocene Supérieur d'Europe. In: Camps, G., Olivier, G. (Eds.), *L'Homme de Cro-Magnon*. Arts et Métiers Graphiques, Paris, pp. 59–72.
- Weber, G.W., Gunz, P., Mitteroecker, P., Stadlmayr, A., Bookstein, F., Seidler, H., 2006. External geometry of Mladec neurocrania compared with anatomically modern humans and Neandertals. In: Teschler-Nicola, M. (Ed.), *Early Modern Humans at the Moravian Gate: The Mladec Caves and their Remains*. Springer, Wien New York, pp. 453–471.
- Wolpoff, M.H., Hawks, J., Frayer, D., Hunley, K., 2001. Modern human ancestry at the peripheries: a test of the replacement theory. *Science* 291, 293–297.
- Yaroch, 1996. Shape analysis using the thin-plate spline: Neanderthal cranial shape as an example. *Am. J. Phys. Anthropol.* 29 (Yrbk), 43–89.